Vietnam Journal of Mechanics, VAST, Vol. 33, No. 2 (2011), pp. 113 – 131

DYNAMIC CHARACTERISTICS OF ELASTICALLY SUPPORTED BEAM SUBJECTED TO A COMPRESSIVE AXIAL FORCE AND A MOVING LOAD

Nguyen Dinh Kien[1], **Le Thi Ha**[2]
[1] *Institute of Mechanics*
[2] *Hanoi University of Transport and Communication*

Abstract. This paper discusses the dynamic characteristics of an elastically supported Euler-Bernoulli beam subjected to an initially loaded compressive force and a moving point load. The eccentricity of the axial force is taken into consideration. The time-histories for beam deflection and the dynamic magnification factors are computed by using the Galerkin finite element method and the implicit Newmark method. The effects of decelerated and accelerated motions on the dynamic characteristics are also examined. The influence of the axial force, eccentricity and the moving load parameters on the dynamic characteristics of the beams is investigated and highlighted.

Keywords: Elastically supported beam, axial force, moving load, Newmark method, dynamic factor.

1. INTRODUCTION

Many structures in practice are subjected to moving loads. Railways, runways, bridges, overhead cranes are typical examples of such structures. Different from other dynamic loads, the position of moving loads varies with time, and this characteristic makes moving load problems a special topic in structural dynamics. Analysis of the moving load problems by using an analytical or a numerical method, thus requires techniques different from that of the conventional dynamic problems.

A large number of researches on moving load problems has been performed. The early and excellent reference is the monograph of Frýba [1], in which a number of closed-form solutions for the moving load problems has been developed by using the Fourier and Laplace transforms. Following the same approach employed by Frýba, in recent years a number of investigations on beams subjected to moving loads has been carried out. Abu-Hilal *et al.* investigated the dynamic response of Bernoulli beam with various boundary conditions subjected to an accelerating and decelerating point load [2], and a harmonic point load [3].

The elastically supported beams exposed to moving loads play an important role in practice, and the dynamic response of the system has been studied extensively. Employing the Fourier transform, Sun constructed the closed-form solutions for the problems of infinite beam resting on a Winkler foundation under line moving loads and harmonic line loads, [4, 5]. Also using the analytical approach, Kim and his co-worker have incorporated the effect of initially leaded axial force and shear deformation on the vibration behavior of infinite beams resting on elastic foundation subjected to a moving harmonic load, [6, 7]. By the same method, Chen and his co-workers studied the effect of foundation viscosity on the dynamic response of beam under moving load, [8]. It is necessary to note that all the above cited work on the elastically supported beam, the beam length is assumed to be infinite, and this assumption prevents the complexity arose by the boundary conditions.

Though the analytical solutions have been obtained for many problems, for more general analyses numerical methods have to be employed. Although moving load problems require some special consideration, the finite element analysis is still a especially powerful method due to its versatility in the spacial discretization. Hino *et al.* seem to be the pioneers in using the finite element method in analyzing moving load problems of bridge engineering, [9, 10]. Lin and Trethewey derived the finite element equations for a Bernoulli beam subjected to moving loads induced by arbitrary movement of a spring-mass-damper system, and then solved the obtained governing equation by the Runge-Kutta integration method, [11]. Thambiratnam and Zhuge computed the dynamic deflection of beams on a Winkler elastic foundation subjected to a constant speed moving load by using the planar 2-node traditional Bernoulli beam element and the direct integration method, and then applied the study to investigation of the railway response, [12]. Also using the direct integration method, Chang and Liu studied the non-linear random vibration of beam resting on an elastic foundation under a moving concentrated load, [13]. Andersen *et al.* described the finite element modelling of infinite Euler beams on Kenvin foundations exposed to moving loads by using the convected co-ordinates, [14]. Wu and Chang investigated the dynamic behavior of a uniform arch under the action of a moving load by deriving an arch element and using the Newmark direct integration method, [15]. Following the standard approach of the finite element analysis and employing the implicit Newmark method in solving governing equations, in recent papers the first author and his co-worker studied the problem of beam resting on a two-parameter elastic foundation subjected to a constant speed moving harmonic load by adopting the Hermite cubic polynomials and the polynomials obtained from the consistent method as interpolation functions, [16, 17]. The influence of the foundation stiffness and moving load parameters on the dynamic deflection of the beam has been investigated in detail in the work.

In this paper, an investigation on the dynamic characteristics of elastically supported beam subjected to a compressive axial force and a moving load is carried out. The moving load considered in this paper is a point load or a harmonic point load with possible type of decelerated and accelerated speed motions. The Galerkin finite element method is employed in derivation of equations of motion, and the implicit Newmark is adopted in computing the dynamic response of the system. Thus, regarding the above cited references, in addition to the Galerkin method employed in deriving the governing equation of an elastically surported beam, some new features are considered in this paper. Firstly,

the effect of eccentricity of the axial force is introduced and studied through a dimensionless parameter. Secondly, the influence of the decelerated and accelerated motions on the dynamic response of the system is investigated for both the two cases of travelling point load and harmonic point load. Furthermore, a detail investigation on the combination effect of the excitation frequency and the travelling speed of the moving load, including the resonant phenomenon is carried out.

Following the above introduction, the remainder of this paper is organized as follow: Section 2 constructs the equations of motion in terms of discretized parameters by using the Galerkin finite element method. Section 3 describes the numerical procedures for computing the nodal load vector and solving the governing equations. Based on the constructed equations and described numerical algorithm, a detail investigation on the effects of the compressive axial force and the loading parameters on the dynamic characteristics is carried out in Section 4. Section 5 summarizes the main conclusions of the paper.

2. GOVERNING EQUATIONS

The problem to be considered herewith is that of transverse vibration of elastically supported pinned-pinned beam subjected to an eccentric compressive force and a moving point load or a moving harmonic point load. The beam is initially loaded by a compressive force P_0, and acted upon by a harmonic point load $f(t) = f_0 \cos \Omega t$, which moves from left to right in a uniform, decelerated or accelerated speed types of motion. With $\Omega = 0$, the moving load resumes to the conventional case of constant magnitude point load. The eccentric compressive load P_0 can be transferred to an axial force P_0 to the center of beam cross-section and a couple $M = P_0 e$, with e is the eccentricity. A sketch of the problem is depicted in Fig. 1.

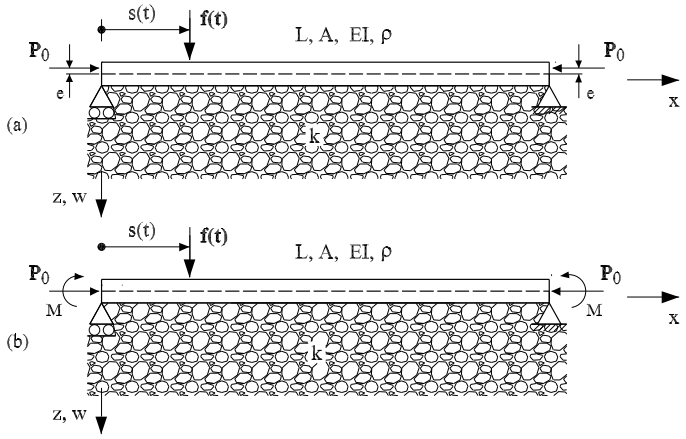

Fig. 1. (a) An elastically supported pinned-pinned beam subjected to an eccentric compressive force and a moving point load; (b) Transferring the eccentric compressive force to the center of the beam cross-section as a compressive axial force and a couple

The differential equation of motion for an Euler-Bernoulli beam subjected to an axial load and a moving point load is given by

$$EI\frac{\partial^4 w(x,t)}{\partial x^4} + m\ddot{w}(x,t) - P_0\frac{\partial^2 w(x,t)}{\partial x^2} + kw(x,t) = p(x,t) \tag{1}$$

where $w(x,t)$ is transverse deflection of the beam (unit of m); EI is the bending stiffness (Nm^2); $m = \rho A$ (ρ and A are the mass density and cross-sectional area, respectively) is the mass per unit of beam length (kg/m); k is the stiffness coefficient of the supporting medium ($\mathrm{N/m}^2$); x is the space coordinate (m); t is the time (s); $\ddot{w}(x,t) = \partial^2 w/\partial t^2$. In the present work, the elastic support is assumed to be modelled by one parameter k, which is in accordance with the classical Winkler model.

The external load $p(x,t)$ in the right hand side of Eq. (1) is defined as

$$p(x,t) = f(t)\,\delta(x - s(t)) = f_0\cos(\Omega t)\,\delta(x - s(t)) \tag{2}$$

with $\delta(.)$ is the Dirac delta function, and $s(t)$ is the function describing the motion of the force $f(t)$ at time t, and given by

$$s(t) = v_0 t + \frac{1}{2}at^2 \tag{3}$$

where v_0 is the initial speed (speed at the left end of the beam), and a is the constant acceleration of the load $p(t)$. For the case of uniform velocity, $a = 0$, and the current position of the moving load is simply as $s(t) = v_0 t$.

The beam is assumed initially at rest with initial conditions given by

$$w(x,0) = 0, \quad \dot{w}(x,0) = \frac{\partial w(x,0)}{\partial t} = 0 \tag{4}$$

The boundary conditions contain both the essential and nonessential ones. The essential boundary conditions for the pinned-pinned beam are as follows

$$w(0,t) = 0, \quad w(L,t) = 0 \tag{5}$$

The nonessential boundary conditions relate to the prescribed moments and transverse shear forces at the beam ends, which having the forms

$$EI\frac{\partial^2 w(x,t)}{\partial x^2} - M_p = 0, \quad EI\frac{\partial^3 w(x,t)}{\partial x^3} - V_p = 0 \quad \text{at } x = 0 \text{ and } x = L \tag{6}$$

where M_p, V_p are the prescribed moments and shear forces, respectively. For the present problem, $V_p = 0$ at both the beam ends.

Following standard procedures of the Galerkin finite element method [18, 19], let the beam be divided into NE elements of length l. Each element has the assumed displacement field $\tilde{w} = \tilde{w}(x,t)$ given by

$$\tilde{w} = [\mathbf{N}]\{\mathbf{d}\} = \sum N_i(x)d_i(t) \tag{7}$$

where $N_i = N_i(x)$, $(i = 1\,..\,4)$ is the weighted functions; d_i is the unknown time functions with nodal values. When Eq. (7) is substituted into Eq. (1), the residual ϵ is given by the

equation difference. In the Galerkin method, one distributes the residual over the spatial domain by using weighting functions N_i and requires that

$$\int_V N_i \epsilon \, dV = 0, \quad i = 1 \,..\, 4 \tag{8}$$

where V is the beam volume. Eq. (8), known as the Galerkin residual equation, shows that the weighting functions are orthogonal to the residual in the domain V. Then, the Galerkin residual equation for a single element with length of l is given by

$$\int_0^l [\mathbf{N}]^T \left(EI \frac{\partial^4 \tilde{w}}{\partial x^4} + m\ddot{\tilde{w}} - P_0 \frac{\partial^2 \tilde{w}}{\partial x^2} + k\tilde{w} - p(x,t) \right) dx = 0 \tag{9}$$

With $EI = \text{const}$, applying integration by parts we get

$$\begin{aligned} \int_0^l [\mathbf{N}]^T EI \frac{\partial^4 \tilde{w}}{\partial x^4} dx &= \int_0^l \left[\frac{\partial^2 \mathbf{N}}{\partial x^2} \right]^T EI \frac{\partial^2 \tilde{w}}{\partial x^2} dx + \left([\mathbf{N}]^T EI \frac{\partial^3 \tilde{w}}{\partial x^3} - \left[\frac{\partial \mathbf{N}}{\partial x} \right]^T EI \frac{\partial^2 \tilde{w}}{\partial x^2} \right) \Big|_0^l \\ &= \int_0^l \left[\frac{\partial^2 \mathbf{N}}{\partial x^2} \right]^T EI \frac{\partial^2 \tilde{w}}{\partial x^2} dx + \left([\mathbf{N}]^T V_p - \left[\frac{\partial \mathbf{N}}{\partial x} \right]^T M_p \right) \Big|_0^l \end{aligned} \tag{10}$$

and

$$-\int_0^l P_0 [\mathbf{N}]^T \frac{\partial^2 \tilde{w}}{\partial x^2} dx = \int_0^l P_0 \left[\frac{\partial \mathbf{N}}{\partial x} \right]^T \frac{\partial \tilde{w}}{\partial x} dx - P_0 [\mathbf{N}]^T \frac{\partial \tilde{w}}{\partial x} \Big|_0^l \tag{11}$$

The last terms in Eq. (10) are determined by the boundary conditions given by the nonessential boundary conditions defined by Eq. (6). In each element, these terms offset by the boundary conditions of the neighboring elements, so that only the boundary condition at the two ends of the beam are necessary. From Eq. (7) we have

$$\dot{\tilde{w}} = [\mathbf{N}]\dot{\mathbf{d}}, \ddot{\tilde{w}} = [\mathbf{N}]\ddot{\mathbf{d}}, \frac{\partial^2 \tilde{w}}{\partial x^2} = [\mathbf{B}]\{\mathbf{d}\} \quad \text{where} [\mathbf{B}] = \left[\frac{\partial^2 \mathbf{N}}{\partial x^2} \right] \tag{12}$$

Substituting Eqs. (7), (10) and (12) into Eq. (9) and assembling elements, we get

$$\begin{aligned} \sum_{j=1}^{NE} \Big\{ &\int_0^l m[\mathbf{N}]^T [\mathbf{N}] dx \{\ddot{\mathbf{d}}\} + \int_0^l [\mathbf{B}]^T EI [\mathbf{B}] dx \{\mathbf{d}\} \\ &+ \int_0^l P_0 \left[\frac{\partial \mathbf{N}}{\partial x} \right]^T \left[\frac{\partial \mathbf{N}}{\partial x} \right] dx \{\mathbf{d}\} + \int_0^l k[\mathbf{N}]^T [\mathbf{N}] dx \{\mathbf{d}\} \Big\} = \mathbf{R}(x,t) \end{aligned} \tag{13}$$

with

$$\mathbf{R}(x,t) = \sum_{j=1}^{NE} \left\{ \int_0^l [\mathbf{N}]^T p(x,t) dx + P_0 [\mathbf{N}]^T \frac{\partial \tilde{w}}{\partial x} \Big|_0^l + \left[\frac{\partial \mathbf{N}}{\partial x} \right]^T M_p \Big|_0^l \right\} \tag{14}$$

Eq. (14) has been written in consideration of that the prescribed shear force V_p is zero at both the beam ends. The summation in the above expressions and hereafter is understood

as the assembly of all elements into the structure by the standard method of the finite element method. Eq. (13) can be written in a familiar form of the finite element analysis

$$[\mathbf{M}]\{\ddot{\mathbf{D}}\} + \big([\mathbf{K}_{\mathrm{B}}] + [\mathbf{K}_{\mathrm{P}}] + [\mathbf{K}_{\mathrm{F}}]\big)\{\mathbf{D}\} = \mathbf{R}(x,t) \tag{15}$$

where

$$[\mathbf{M}] = \sum_{j=1}^{NE} \int_0^l m[\mathbf{N}]^T[\mathbf{N}]dx, [\mathbf{K}_{\mathrm{B}}] = \sum_{j=1}^{NE} \int_0^l [\mathbf{B}]^T EI[\mathbf{B}]dx \tag{16}$$

are the mass and stiffness matrices of the beam, respectively;

$$[\mathbf{K}_{\mathrm{P}}] = \sum_{j=1}^{NE} \int_0^l P_0 \left[\frac{\partial \mathbf{N}}{\partial x}\right]^N \left[\frac{\partial \mathbf{N}}{\partial x}\right] dx \tag{17}$$

is the geometric stiffness matrix, resulted from the effect of the initially loaded axial force, and

$$[\mathbf{K}_{\mathrm{F}}] = \sum_{j=1}^{NE} \int_0^l k[\mathbf{N}]^T[\mathbf{N}]dx \tag{18}$$

is the stiffness matrix stemming from the foundation deformation.

3. SOLUTION PROCEDURES

As seen from Eqs. (15) - (18), in order to compute the nodal load vector as well as the mass and stiffness matrices, we need to introduce expressions for the weighted functions N_i. In the the present work, the following Hermite polynomials are employed for this purpose

$$\begin{aligned} N_1 &= 1 - 3\frac{x^2}{l^2} + 2\frac{x^3}{l^3}; \quad & N_2 &= x - 2\frac{x^2}{l} + \frac{x^3}{l^2} \\ N_3 &= 3\frac{x^2}{l^2} - 2\frac{x^3}{l^3}; & N_4 &= -\frac{x^2}{l} + \frac{x^3}{l^2} \end{aligned} \tag{19}$$

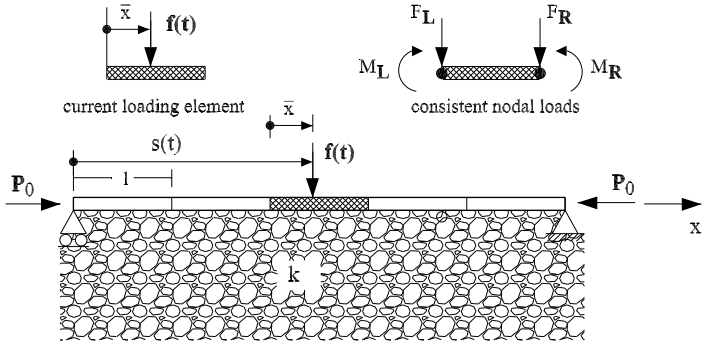

Fig. 2. Current loading position of travelling load and element consistent nodal loads

The abscissa x of the weighted function N_i in Eq. (19) is measured from the left node of the current loading element, and for a mesh of equal-length elements, this abscissa is computed as (conf. Fig. 2 and Eq. (3))

$$x = s(t) - (n-1)l = v_0 t + \frac{1}{2}at^2 - (n-1)l \tag{20}$$

where n is the number of the element on which the load $f(t)$ is acting, and t is the current time. Having the abscissa x determined, the weighted functions N_i are completely known. It is necessary to note that the travelling load results in a non-zero nodal load vector for the element under loading. In this regards, the first term in the expression of the nodal load vector, Eq. (14), is the consistent load vector, having the form

$$\begin{aligned}\sum_{j=1}^{NE}\int_0^l [\mathbf{N}]f(x,t)dx &= \left\{0\ 0\ 0\ ...\ \underbrace{\int_0^l [\mathbf{N}]f(x,t)dx}_{\text{current loading element}}\ ...\ 0\ 0\ 0\right\}^T \\ &= \left\{0\ 0\ 0\ ...\ \underbrace{F_L\ M_L\ F_R\ M_R}_{\text{current loading element}}\ ...\ 0\ 0\ 0\right\}^T\end{aligned} \tag{21}$$

where the loads and moments at the left and right nodes of the current loading element are given by

$$\begin{aligned} F_L &= N_1|_x\, f_0\cos(\Omega t)\ ; \quad M_L = N_2|_x\, f_0\cos(\Omega t) \\ F_R &= N_3|_x\, f_0\cos(\Omega t)\ ; \quad M_R = N_4|_x\, f_0\cos(\Omega t)\end{aligned} \tag{22}$$

where $N_i|_x$ denotes the expression of weighted function N_i evaluated at the current load position, the abscissa x, defined by Eq. (20). Thus, Eqs. (14), (21) and (22) completely define the nodal load vector of the structure at current time t.

The equations of motion (15) can be solved by the implicit Newmark family of methods, which ensures unconditionally numerical stable and has no restriction on the time step size. The average acceleration method is adopted in the present work. The details of the implicit Newmark family of methods as well as the method of choosing time step to ensure the accuracy are described in [18, 20].

4. NUMERICAL RESULTS AND DISCUSSIONS

To investigate the dynamic characteristics of the elastically supported beam subjected to an eccentric compressive force and a moving load, the following material and geometric data are adopted:

$L = 20$ m; $I = 0.0234$ m^4; $E = 30 \times 10^9$ N/m^2;
$m = 1000$ kg/m; $f_0 = 100 \times 10^3$ N; $k = 4 \times 10^5$ N/m^2

The above chosen value of the parameter k represents a sandy-clay foundation, [21]. However, in order to determine this parameter for a practical foundation, the standard experimental procedures are necessary to carry out. To examine the effect of the eccentricity,

the beam cross section is assumed to be rectangular with height h. The computations are carried out by using 20 elements with length of 0.5 m, and 100 time steps.

4.1. Constant speed point load

This subsection investigates the dynamic characteristics of the beam subjected to an initially loaded axial force and a constant speed point load, $v = v_0 = \text{const}, a = 0$. To verify the derived formulations and developed computed code, the time histories for normalized mid-span deflection of the beam without elastic support are computed, and the results are depicted in Fig. 3a. In the figure, w_0 is the static mid-span deflection, and ΔT is the total time needed for the load to move completely from the left end to the right end of the beam; α is the speed parameter, defined as a ratio of the load speed to the critical speed of the unsupported beam, $\alpha = v/v_{cr}$, with $v_{cr} = L\omega_1/\pi$ (ω_1 is the first natural frequency of the beam), [22]. It can clearly see from Fig. 3a that the time histories of the beam without elastic support obtained in the present work are in excellent agreement with the exact solutions reported in Ref. [22].

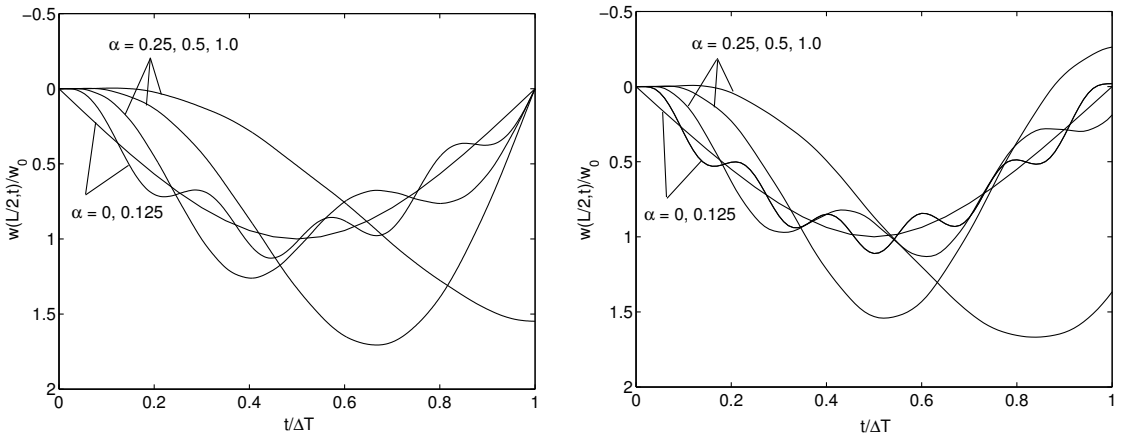

(a) $k = 0, P_0 = 0$ (b) $k = 4 \times 10^5$ N/m^2, $P_0 = 0$

Fig. 3. Time histories for normalized mid-span deflection of beam subjected to a constant speed point load: (a) without elastic support, (b) with elastic support

Fig. 3b shows the time histories for normalized mid-span deflection of the elastically supported beam subjected to a moving point load with the same speeds as the case of Fig. 3a. By comparing Fig. 3a and Fig. 3b, some difference in the dynamic response of the unsupported beam and elastically supported beam can be observed. The curves for $\alpha = 0.125$ and $\alpha = 0.25$ of the elastically supported beam oscillate more about the static influence line (the dash lines in the figures with $\alpha = 0$). For example, with $\alpha = 0.125$ the unsupported beam executes four cycles of the important lowest vibration mode, while the elastically supported beam performs five and half cycles. This phenomenon can be understood as the elastically supported beam is a stiffer system comparing to the unsupported one. As a result, the natural frequency of the supported beam is higher than

that of the unsupported beam. For $\alpha < 1$ the mid-span deflection of the unsupported beam is zero when the load exits the beam, but this is not true for the elastically supported beam. With the speeds under investigation, the mid-span deflection of the elastically supported beam is not zero when the load exits the beam, and it can be positive or negative, depends on the travelling speed. The negative mid-span deflection is possible due to the beam is under vibration. Furthermore, at a give time speed, the maximum response of the elastically supported beam occurs at an earlier time than that of the unsupported beam. Table 1 lists the dynamic magnification factors f_D of the elastically supported

Table 1. The dynamic magnification factor f_D for elastically supported beam at various values of travelling speed and axial force

	P_0/P_E			
v (m/s)	0	0.2	0.4	0.6
20	1.0680	1.1239	1.1734	1.1762
40	1.1356	1.2401	1.3626	1.5242
60	1.4759	1.5583	1.6433	1.7219
80	1.6493	1.6839	1.7232	1.7247
100	1.7038	1.7181	1.7031	1.6464
110	1.7025	1.7097	1.6804	1.5848
120	1.6893	1.6886	1.6479	1.5176

beam at various values of the travelling load speed and the axial force. In the table and hereafter, the dynamic magnification factor is defined as the ratio of the maximum of the mid-span dynamic deflection to the mid-span static deflection, $f_D = \max(w(L/2,t)/w_0)$; $P_E = 3.3533 \times 10^7$ N is the Euler buckling load of the elastically supported beam, which can be obtained by solving the following eigenvalue problem

$$([\mathbf{K}_\mathrm{B}] + [\mathbf{K}_\mathrm{F}] + P_E[\mathbf{K}_\mathrm{P}])\{\mathbf{D}\} = \{\mathbf{0}\} \tag{23}$$

It is necessary to note that by writing the eigenvalue problem in the form (23), the axial force P_0 in the stiffness matrix $\mathbf{K}_\mathrm{P}$, Eq. (17), should be omitted

It can be seen from Table 1 that with the presence of the axial force, the dynamic magnification factor is more sensitive to the speed of the travelling load. For a higher value of the axial force, the maximum dynamic magnification factor tends to be reached at a lower travelling speed. The phenomena may be resulted from the reduction in the bending stiffness of the beam due to presence of the compressive axial force, as explained in [23]. Furthermore, at a given speed of the travelling load, the maximum response, as seen from Fig. 4, occurs at a later time when the axial force is larger. In an extraordinary case with $P_0 = 0.6P_E$ and $v = 120$ m/s, the maximum response occurs after the load exits the beam.

The time-history for the mid-span deflection of the elastically supported beam at various values of the eccentricity and the moving speed are depicted in Fig. 5 for the case $P_0 = 0.2P_E$. The dynamic magnification factors of the beam at various values of the eccentricity and the axial force for two cases $v = 20$ m/s and $v = 60$ m/s are listed in Table 2. The effect of the eccentricity is clearly seen from the figure and the table. Firstly,

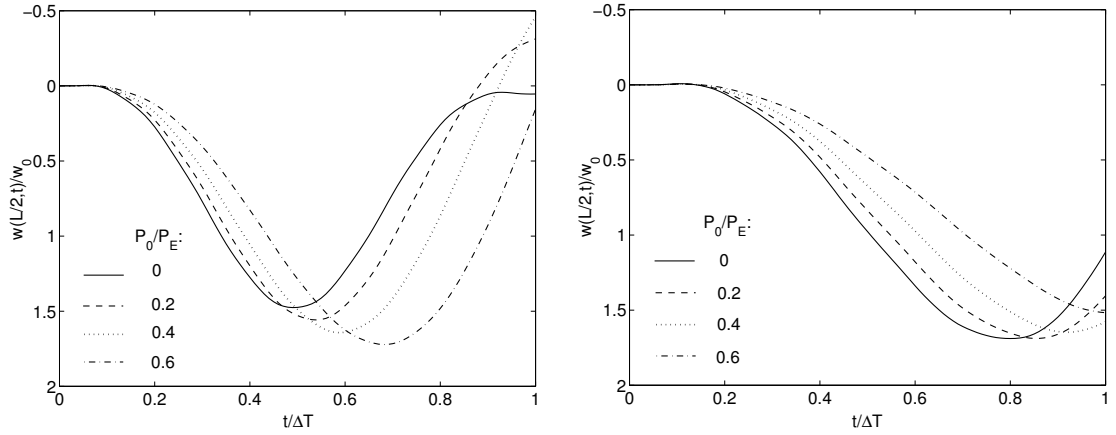

(a) v = 60 m/s, $e = 0$ (b) v = 120 m/s, $e = 0$

Fig. 4. Time histories for normalized mid-span of elastically supported beam under constant speed point load with various values of axial force

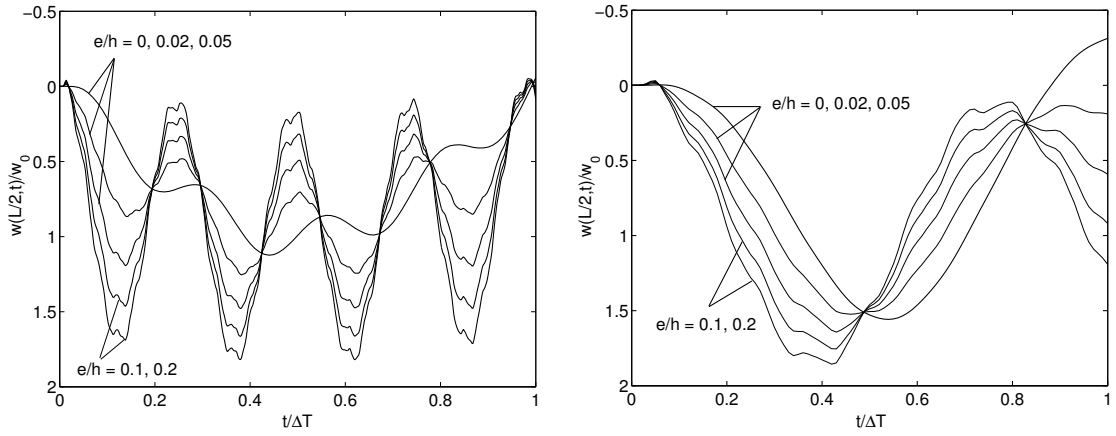

(a) v = 20 m/s, $P_0 = 0.2P_E$ (b) v = 60 m/s, $P_0 = 0.2P_E$

Fig. 5. Time histories for normalized mid-span deflection of elastically supported beam subjected to an axial force and a constant speed point load at various values of eccentricity

at the given value of the axial force, the maximum dynamic deflection gradually increases with an increment in the eccentricity, regardless of the travelling speed. Secondly, with the presence of the eccentricity, the curves for the mid-span deflection are no longer smooth, and at some points the sudden change in the dynamic deflection is observed. This effect suggests that the eccentricity plays a similar role as a shock on the dynamic response of

Table 2. The dynamic magnification factor for elastically supported beam subjected to a constant speed point load at various values of axial force and eccentricity

		P_0/P_E		
v (m/s)	e/h	0.2	0.4	0.6
20	0.02	1.2627	1.4589	1.5710
	0.05	1.4738	1.6824	1.7780
	0.10	1.6597	1.8277	1.8898
	0.20	1.8144	1.9289	1.9597
60	0.02	1.5243	1.6579	1.7905
	0.05	1.6426	1.7840	1.8970
	0.10	1.7546	1.9002	1.9567
	0.20	1.8565	1.9821	1.9940

the beam. The number of cycles of the lowest vibration mode which the beam executed, as seen from Fig. 5, is unchanged by the eccentricity, regardless of the travelling speed.

4.2. Constant speed harmonic load

This subsection investigates the dynamic characteristics of the elastically supported beam subjected to a compressive force P_0 and and a harmonic load $f = f_0 \cos(\Omega t)$ travelling with a constant speed $v = v_0 = \text{const}$. The influence of the travelling speed, excitation frequency of the moving load as well as the axial force and eccentricity on the dynamic response of the beam is examined.

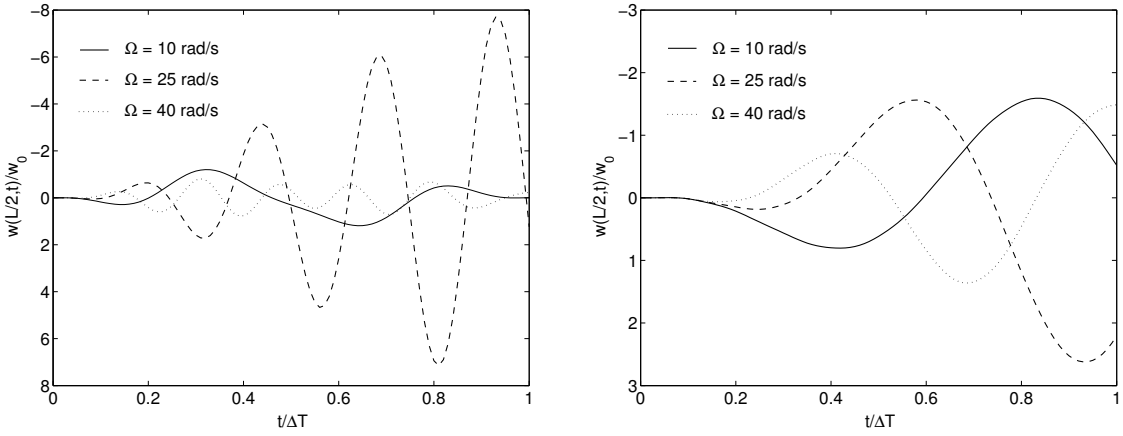

(a) v = 20 m/s, $P_0 = 0.2P_E$ (b) v = 60 m/s, $P_0 = 0.2P_E$

Fig. 6. Time histories for normalized mid-span deflection of elastically supported beam subjected to an axial load and a harmonic point load with various values of excitation frequency

Fig. 6 displays the time histories for normalized mid-span deflection of the elastically supported beam subjected to an axial load and a harmonic point load with various values of the excitation frequency for two travelling speeds $v = 20$ m/s and $v = 60$ m/s. It is noted that the fundamental vibration frequency of the elastically supported beam initially loaded by a compressive axial force $P_0 = 0.2P_E$ is 25.7275 (rad/s). Thus, the excitation frequency chosen for the study is well below, considerable above and very near the fundamental frequency. The effect of the excitation frequency and the moving speed on the dynamic characteristics can be observed clearly from the figure. With $\Omega = 40$ rad/s, the maximum response is considerably lower than that obtained for $\Omega = 10$ rad/s and $\Omega = 25$ rad/s, and a higher excitation frequency is, the more cycles of the lowest vibration mode the beam tends to execute, regardless of the moving speed. The resonant effect is clearly observed at the low travelling speed, but this effect is considerably reduced at the high moving speed. With $\Omega = 25$ rad/s, the dynamic magnification factor is 7.7053 and 2.6222 respectively for the moving speed $v = 20$ m/s and $v = 60$ m/s, which is very different.

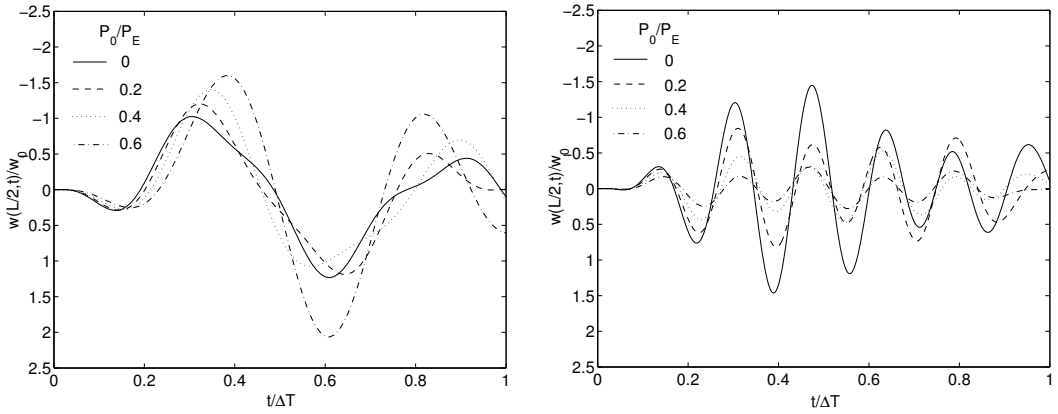

(a) v = 20 m/s, $\Omega = 10$ m/s (b) v = 20 m/s, $\Omega = 40$ m/s

Fig. 7. Effect of axial force on dynamic response of elastically supported beam subjected to a constant speed harmonic point load at various values of axial force

Fig. 7 illustrates the effect of the axial force on the dynamic response of the elastically supported beam subjected to a constant speed harmonic point load for two cases of the excitation frequency, $\Omega = 10$ rad/s and $\Omega = 40$ rad/s. The fundamental frequencies of the system with $P_0/P_e = 0, 0.2, 0.4, 0.6$ are 28.7643, 25.7275, 22.2807 and 18.1921 rad/s, respectively. Thus, the choosing frequencies for the investigation are well below and considerable above the fundamental frequencies. When the excitation frequency is lower than the fundamental frequency, the dynamic deflection of the beam is considerably increased with the presence of the compressive axial force, and a higher compressive force is, a larger dynamic deflection is (conf. Fig. 7a). This effect of the compressive force on the structural behavior is similar to the case of quasi-static loading, in which the compressive axial force reduces the bending stiffness of the beam structures as mentioned above, and the beam deflection increases with an increment in the compressive axial force. On the contrary, the

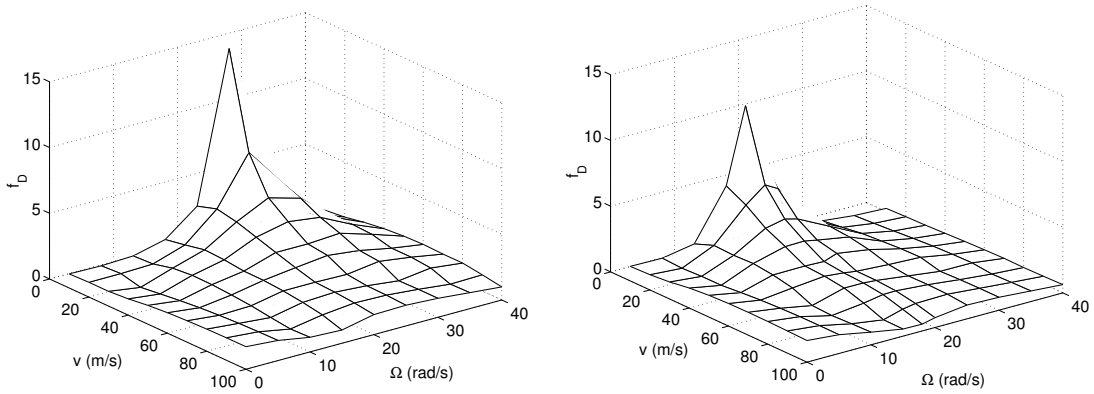

(a) $P_0 = 0.2P_E$ (b) $P_0 = 0.6P_E$

Fig. 8. Speed and excitation frequency versus dynamic magnification factor of elastically supported beam subjected to a constant speed harmonic load

presence of the compressive axial force reduces the dynamic deflection of the beam when the excitation frequency is higher than the fundamental frequency. The influence of the moving speed and excitation frequency on the magnification factor is displayed in Fig. 8. The figure shows a clear resonant effect, especially with the travelling speed $v \leq 30$ m/s. Though the higher axial force results in higher magnification factor for the speed $v \leq 40$ m/s, the effect of the resonance is remarkable reduced with the high value of the axial force. The numerical results obtained in this subsection show the important role of the moving speed, the excitation frequency and the axial force on the dynamic characteristics of the elastically supported beam subjected to a constant speed harmonic point load. The resonant phenomenon is less important at the high moving load speed, and at the large axial force.

Similar to the case of constant speed point load, the dynamic deflection of the elastically supported beam subjected to a constant speed harmonic point load increases with an increment in the eccentricity, regardless of the excitation frequency, Fig. 9. For higher values of the moving speed and the axial force (not shown herewith), the tendency is the same as the case of $v = 20$ m/s and $P_0 = 0.2P_E$ in Fig. 9. Thus, in addition to the increment in the dynamic deflection, the eccentricity results in a sudden change in this parameter. No change in the vibration period is observed either with the presence and increment in the eccentricity.

4.3. Decelerated and accelerated motions

This subsection studies the influence of decelerated and accelerated motions on the dynamic characteristics of the elastically supported beam. In the decelerated motion, speed of the travelling load at the left end of the beam is assumed to be v, and it is zero at the right end of the beam. For the case of the accelerated motion, the speed at these ends is zero and v, respectively. The time histories and the dynamic magnification factor of the elastically supported beam under these motions are examined.

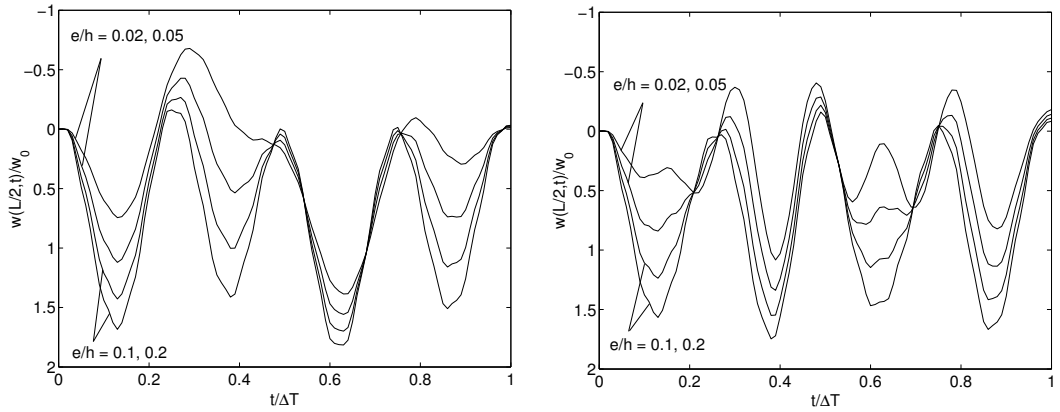

(a) v = 20 m/s, $\Omega = 10$ m/s (b) v = 20 m/s, $\Omega = 40$ m/s

Fig. 9. Effect of eccentricity on dynamic response of elastically supported beam subjected to a compressive axial force ($P_0 = 0.2P_E$), and a constant speed harmonic point load

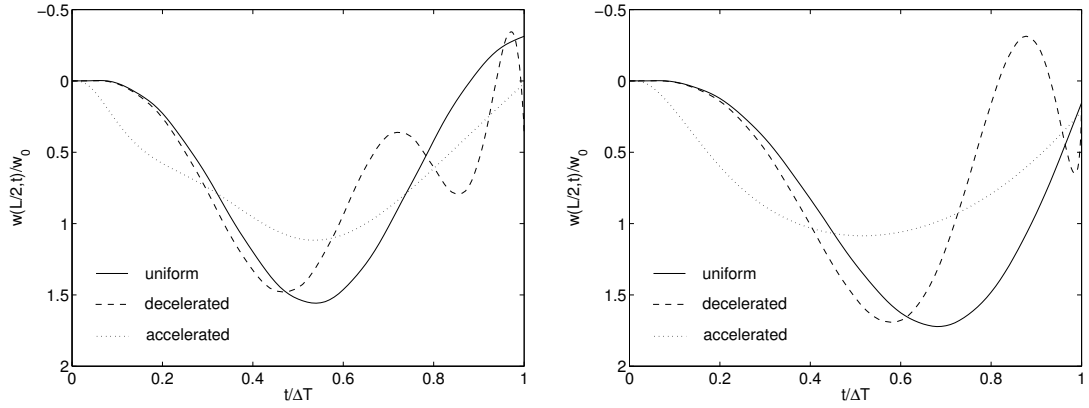

(a) $v = 60$ m/s, $P_0 = 0.2P_E$ (b) $v = 60$ m/s, $P_0 = 0.6P_E$

Fig. 10. Influence of decelerated and accelerated motions on dynamic response of the elastically supported beam subjected to a compressive axial force and a moving point load

The influence of the decelerated and accelerated motions on dynamic response of the elastically supported beam subjected to a compressive axial force and a moving point load with a travelling speed $v = 60$ m/s is depicted in Fig. 10 for two values of the axial force $P_0 = 0.2P_E$ and $P_0 = 0.6P_E$. The corresponding curves for the beam subjected to a compressive axial force and a moving harmonic point load are shown in Fig. 11. A noticeable change in the maximum dynamic response of the beam by the motions is observed. The dynamic magnification factor for the curves in Fig. 10a is 1.5583, 1.4798 and

1.1171 for the uniform, decelerated and accelerated motions, respectively. This factor for the curves in Fig. 10b is 1.7219, 1.6916 and 1.0860. Thus, for the given speeds, the dynamic magnification factor is slightly changed by the decelerated motion, and remarkably reduced by the accelerated motion. This tendency is similar for the case of the harmonic point load (conf. Fig. 11). Furthermore, under decelerated motion the beam subjected to the point load tends to vibrate more than the two other cases. It is noted that the total time necessary for the load completely travelling through the beam in case of the decelerated motion is longer comparing to the case of the uniform motion. The longer travelling time plus the earlier vibration effect due to high speed of the load at the beginning may be the reason of the more numbers of vibration cycles which the beam executed in the the decelerated motions as shown in Fig. 10. The dynamic response in case of the moving harmonic load is completely different under the accelerated motion: the mid-span deflection of the beam under the decelerated motion is the same direction with that of the uniform motion, while the deflection under the accelerated motion is in an opposite side, regardless of the excitation frequency.

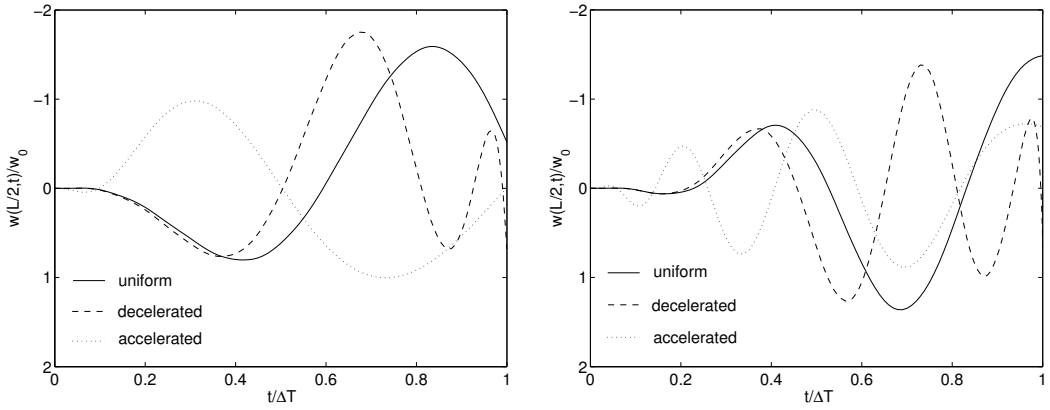

(a) $v = 60$ m/s, $\Omega = 10$ rad/s (b) $v = 60$ m/s, $\Omega = 40$ rad/s

Fig. 11. Influence of decelerated and accelerated motions on dynamic response of the elastically supported beam subjected to an axial force ($P_0 = 0.2P_E$) and a moving harmonic point load

To study the effects of the moving load parameters on the dynamic magnification factor, the computation has been performed with various values of the moving speed and the excitation frequency (in case of the moving harmonic load). The travelling speed of the moving point load versus the dynamic magnification factor is depicted in Fig. 12 for two values of the axial force, $P_0 = 0.2P_E$ and $P_0 = 0.6P_E$. One can see that at the low speed, the magnification factors in Fig. 12 both increase and decrease with increasing the moving speed v. This phenomenon is associated with the oscillations as discussed above and in [22]. The magnification factor obtained in the uniform speed motion is higher than that of other motion types when $v \leq 85$ m/s for $P_0 = 0.2P_E$, and $v \leq 65$ m/s for $P_0 = 0.6P_E$. Beyond these speeds, the dynamic magnification factor of uniform speed motion is smaller

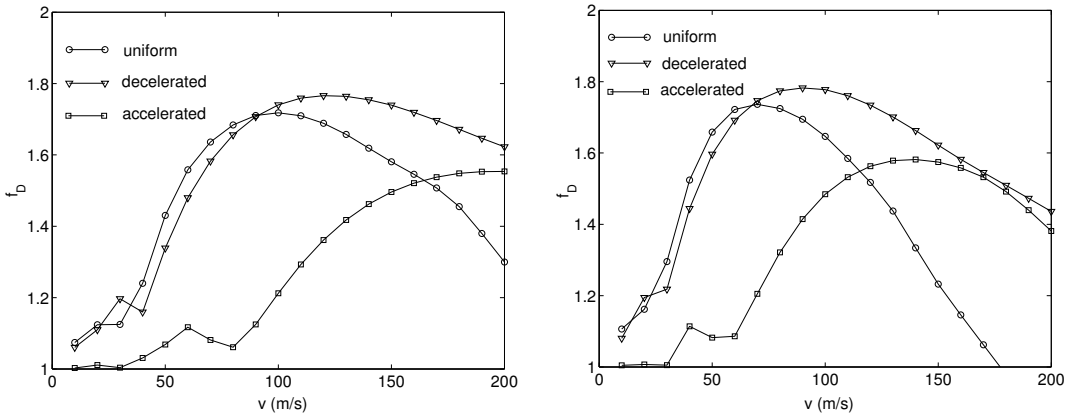

(a) $P_0 = 0.2P_E$ (b) $P_0 = 0.6P_E$

Fig. 12. Travelling speed versus dynamic magnification factor of elastically supported beam under a moving point load

than that of the decelerated motion, and the difference between these factors is more pronounced at the higher speed. The dynamic magnification factor of the accelerated motion is higher than that of the uniform motion only in case of very high speed, namely $v \geq 165$ m/s and $v \geq 115$ m/s for $P_0 = 0.2P_E$ and $P_0 = 0.6P_E$, respectively. The total travelling time in case of the uniform motion is less than that in case of the decelerated and accelerated motions, and at the high moving speed the total travelling time is too short for the maximum response to occur (Conf. Fig. 3). As a result, the dynamic factor in the uniform motion obtained in case of the high moving speed is less than that in case of the accelerated motion. These high speeds, however rarely occur in practice, and thus from practical point of view the accelerated motion is less important than the two other cases.

The speed and excitation frequency versus the dynamic magnification factor of the elastically supported beam subjected to a harmonic point load with different types of motion is displayed in Fig. 13 for the case of centric axial force $P_0 = 0.2P_E$. The resonant effect is clearly seen from the figure, and the dynamic magnification factors obtained with $\Omega = 25$ rad/s, which is very near the fundamental frequency is remarkably high, regardless of the motion types. The maximum magnification factor obtained in the decelerated motion is slightly higher than that of the accelerated motion. The effect of the resonance is more serious at the low speed, and it is less important for the high speed. For $\Omega = 25$ rad/s, the magnification factor obtained in case of the decelerated motion at speed $v = 100$ m/s is 2.3951, which is much lower that 13.2897 at speed $v = 10$ m/s. For the accelerated motion, this factor is 12.6140 and 1.9459 for $v = 100$ m/s and $v = 10$ m/s, respectively.

Fig. 14 shows the moving speed versus the dynamic response of the elastically supported beam subjected to a moving point load with different motions and eccentricities. In the decelerated motion, the dependence of the magnification factor on the moving speed is similar to that of the centric beam, and the factor is higher for a larger eccentricity. The

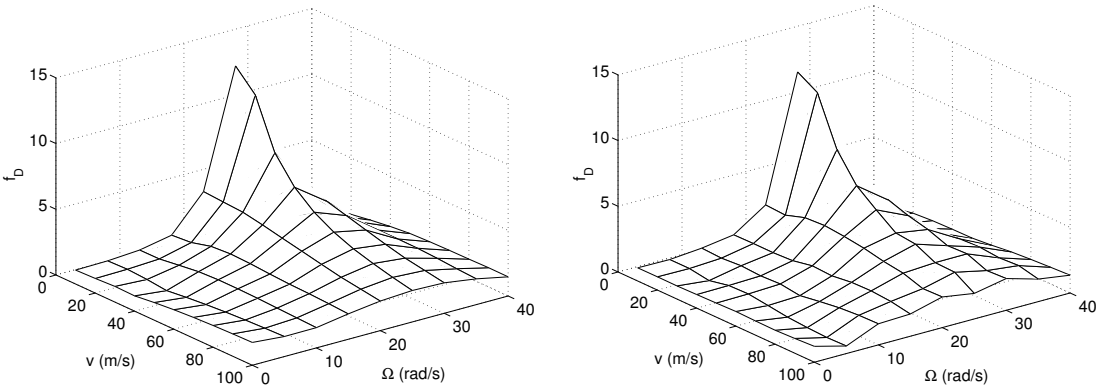

(a) decelerated (b) accelerated

Fig. 13. Speed and excitation frequency versus dynamic magnification factor of elastically supported beam subjected to a harmonic point load with different types of motion ($P_0 = 0.2P_E, e = 0$)

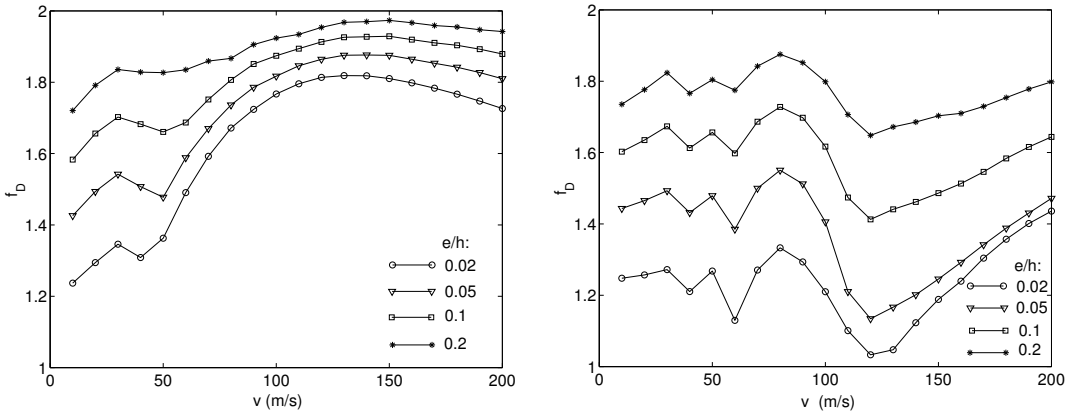

(a) decelerated motion (b) accelerated motion

Fig. 14. Moving speed versus dynamic response of elastically supported beam subjected to a moving point load with different motions and eccentricities

effect of the eccentricity on the magnification factor in the accelerated motion is very different. For the speed $v \leq 130$ m/s, the factor both increases and decreases with increasing the moving speed, and this phenomenon may be caused by the oscillation of the beam in the accelerated motion at this speed. The influence of the excitation frequency frequency and eccentricity on the magnification factor of the beam exposed to a harmonic point load (not shown herewith) is more complex, and it is governed by the excitation frequency.

5. CONCLUDING REMARKS

The paper investigated the dynamic characteristics of elastically supported beam subjected to an eccentric compressive axial force and a moving point load. The equations of motion for the system have been constructed by using the Galerkin finite element method. The time histories for normalized mid-span deflection and the dynamic magnification factor have been computed by using the implicit Newmark method. The effects of the loading parameters and the axial force, including the eccentricity on the dynamic characteristics of the beam have been investigated in detail. Some main conclusions of the paper are as follows.

- The maximum dynamic response of the elastically supported beam under a constant speed point load occurs at a lower moving speed with the presence of the axial force. At a given moving speed, a higher axial force is, a later time the maximum response occurs.

- The effect of the axial force on the dynamic characteristics of the elastically supported beam subjected to a moving harmonic load is governed by the excitation frequency. When the excitation frequency is lower than the fundamental frequency, an increment in the axial force leads to an increment in the maximum dynamic deflection. In contrast, when the excitation frequency is higher than the fundamental frequency, a reduction in maximum dynamic response is observed by increasing in the axial force.

- Resonant effect of the beam exposed to a harmonic load depends on the moving speed and the axial force amplitude. This effect is less important at the high values of the moving speed and the axial force.

- An increment in the eccentricity results in an increment in the maximum dynamic response for both the cases of the constant speed point load and the constant speed harmonic load.

- The influence of the decelerated and accelerated motions on the dynamic magnification factor of the beam subjected to a moving point load depends on the moving speed. In practice, the magnification factor of the accelerated motion is usually smaller than that of the two remaining motions.

- The effect of the resonance on the magnification factor is slightly changed in the decelerated motion, but it is remarkably reduced in accelerated motion. The effect is less important at the high moving speed.

- In the decelerated motion, the magnification factor of the beam subjected to a point load increases with increasing eccentricity as in case of centric axial force. In the accelerated motion, this factor is different from that of the centric axial load.

REFERENCES

[1] L. Fryba, Vibration of solids and structures under moving loads, *Academia, Prague*, (1972).

[2] M. Abu-Hilal and H. S. Zibden, Vibration of beams with general boundary traversed by a moving force, *Journal of Sound and Vibration*, **229** (2000) 377 - 388.

[3] M. Abu-Hilal and M. Mohsen, Vibration of beams with general boundary conditions due to a moving harmonic load, *Journal of Sound and Vibration*, **232** (2000) 703 - 717.

[4] L. Sun, Dynamic displacement response of beam-type structures to moving line loads, *International Journal of Solids and Structures*, **38** (2001) 8869 - 8878.

[5] L. Sun, A closed form solution of a Bernoulli-Euler beam on a viscoelastic foundation under harmonic line loads, *Journal of Sound and Vibration*, **242** (2001) 619 - 627.
[6] S.M. Kim, Vibration and stability of axial loaded beams on elastic foundation under moving harmonic loads, *Engineering Structures*, **26** (2004) 95 - 105.
[7] S.M. Kim and Y.H. Cho, Vibration and dynamic buckling of shear beam-column on elastic foundation under moving harmonic loads, *International Journal of Solids and Structures*, **43** (2006) 393 - 412.
[8] Y.H. Chen and Y.H Huang and C.T. Shin, Response of an infinite Timoshenko beam on a viscoelastic foundation to a harmonic moving load, *Journal of Sound and Vibration*, **241** (2001) 809 - 824.
[9] J. Hino, T. Yoshimura, K. Konihi and N. Ananthanarayana, A finite element method prediction of the vibration of a bridge subjected to a moving vehicle load, *Journal of Sound and Vibration*, **96** (1984) 45 - 53.
[10] J. Hino, T. Yoshimura, and N. Ananthanarayana, Vibration analysis of non-linear beams subjected to a moving load using the finite element method, *Journal of Sound and Vibration*, **100** (1985) 477 - 491.
[11] W.H. Lin and M.W. Trethewey, Finite element analysis of elastic beams subjected to moving dynamic loads, *Journal of Sound and Vibration*, **136** (1990) 323 - 342.
[12] D. Thambiratnam and Y. Zhuge, Dynamic analysis of beams on elastic foundation subjected to moving loads, *Journal of Sound and Vibration*, **198** (1996) 149 - 169.
[13] T.P. Chang and Y.N. Liu, Dynamic finite element analysis of a nonlinear beam subjected to a moving load, *International Journal of Solids and Structures*, **33** (1996) 1673 - 1688.
[14] L. Andersen, S.R.K. Nielsen and P.H. Kirkegaard, Finite element modelling of infinite Euler beams on Kelvin foundations exposed to moving load in convected co-ordinates, *Journal of Sound and Vibration*, **241** (2001) 587 - 604.
[15] J.S. Wu and L.K. Chang, Dynamic analysis of an arch due to a moving load, *Journal of Sound and Vibration*, **269** (2004) 511 - 534.
[16] Nguyen Dinh Kien and Tran Thanh Hai, Dynamic analysis of prestressed Bernoulli beams resting on two-parameter foundation under moving harmonic load, *Vietnam Journal of Mechanics*, **28** (2006) 176 - 188.
[17] Nguyen Dinh Kien, Dynamic response of prestressed Timoshenko beams resting on two-parameter foundation to moving harmonic load, *Technische Mechanik*, **28** (2008) 237 - 258.
[18] R.D. Cook, D.S. Malkus and M.E. Plesha, Concepts and applications of finite element analysis, *Third Ed., John Wiley & Sons, New York*, (1989).
[19] G. Strang, Introduction to applied mathematics, *Wellesley-Cambridge Press, Wellesley, Massachusetts*, (1986).
[20] M. Géradin and R. Rixen, Mechanical vibrations. Theory and application to structural dynamics, *Second Ed., John Wiley & Sons, Chichester*, (1997).
[21] Z. Feng and R.D. Cook, Beam elements on two-parameter elastic foundations, *Jounal of Engineering Mechanics, ASCE*, **109** (1983) 1390 - 1402.
[22] M. Olsson, On the fundamental moving load problem, *Journal of Sound and Vibration*, **145** (1991) 299 - 307.
[23] A. Ghali and A.M. Neville, Structural analysis. A unified classical and matrix approach, *Third Ed., E & FN Spon, London*, (1995).

Received January 5, 2010